ISBN: 978-3-95450-227-1 ISSN: 2673-5490 doi:10.18429/JACoW-IPAC2022-THPOTK032

A VACUUM SYSTEM FOR THE MILLIAMPERE BOOSTER*

R. Heine, C. Lorey
Institut für Kernphysik, Johannes Gutenberg-Universität Mainz,
D-55099 Mainz, Germany

Abstract

The Milliampere Booster (MAMBO) is the injector linac for the Mainz Energy-recovering Superconducting Accelerator MESA. MESA is a multi-turn energy recovery linac with beam energies in the 100 MeV regime currently designed and built at Institut für Kernphysik (KPH) of Johannes Gutenberg-Universität Mainz [1]. The main accelerator consists of two superconducting Rossendorf type modules [2–4], while the injector MAMBO [5] relies on normal conducting technology. The four MAMBO radio frequency cavities are bi-periodic $\pi/2$ structures [6,7] that are about 2 m long, each. In this paper we present the results of Molflow+ [8] simulations of several setups of the vacuum system for MAMBO that differ in number of pumps, pumping speed and diameter of the pumping ports that are connected to the DN40 beam pipe.

INTRODUCTION

The MESA facility is a few turn recirculating electron linac that can be operated in two modes. The first mode is called external mode where a beam of polarised electrons at $T = 155$ MeV and up to $I = 150\,\mu$A ($Q = 0.12$ pC) is lead onto the target of the P2-experiment [9] and dumped afterwards. The second mode is the energy recovery mode for the MESA gas internal target experiment (MAGIX) [10]. Here a beam of $I = 1$ mA ($Q = 0.77$ pC) of non polarised electrons is recovered from $T = 105$ MeV to injection energy ($T = 5$ MeV) after interaction with the target. For MESA stage-II the beam current delivered to MAGIX will be increased to 10 mA ($Q = 7.7$ pC).

Two main components of MESA are quite susceptible to high vacuum pressure: the superconducting cavities of the main linac and the photo cathodes of the particle sources. Therefore it was agreed to have stainless steel chambers with ConFlat (CF) flanges to achieve ultra high vacuum (UHV). The beam pipe diameter was set to DN40.

MAMBO comprises of four copper cavities of approx. 2 m length that are connected by three drifts of 1 m length that contain ion getter pumps (IGP). The first cavity has 37 cells, the other three have 33 cells. The cells are separated by copper webs that incorporate two coupling slots and the beam port. In a bi-periodic structure there are two types of cells, a long one that accelerates the beam and a short one that couples the field. The later one being about 10 % of $\lambda_{RF}/2$ long, and the first one $\approx 0.9\lambda_{RF}/2$. The cavities are pumped by the drifts via the beam ports. The cavities are expected to act like a differential pumping stage. Because of their geometry, analytical vacuum calculations are complicated and therefore numerical simulations with the Molflow+ code [8] were carried out.

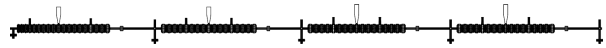

(a) One IGP per drift with DN40 pipes on LUMOs (in total five IGPs).

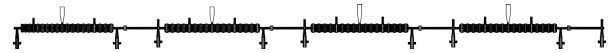

(b) Two IGPs per drift with DN63 pipes on LUMOs and a T-crosses (in total nine IGPs).

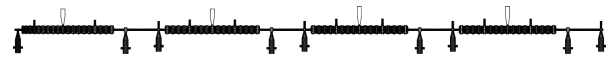

(c) Two IGPs per drift with DN100 pipes on LUMOs and PIMOs (in total nine IGPs).

Figure 1: Examples of vacuum geometries used for the Molflow+ simulations. Beam direction is from left to right.

VACUUM SETUPS

Initially vacuum pumps at the entrance of each cavity were foreseen. From the analytical formulas (e.g. [11]), it was expected that the DN40 beam pipe would limit pumping and therefore a pumping speed of $S_0 \approx 35$ L/s would be sufficient.

This starting point was expanded to three IGP sizes ($S_0 = 35$ L/s, 60 L/s and 90 L/s) and three sizes of pumping ports (CF40, CF63 and CF100). The pumps were connected to the beam pipe at a spare CF40 flange of a screen monitor (LUMO) acting as a T-chamber followed by a 150 mm straight chamber (see Fig. 1(a)) or one that tapers from DN40 to DN63 or DN100, respectively.

Further configurations with two IGPs comparable to the one shown in Fig. 1(b) were investigated. Those setups allow pumping of the cavities from both beam ports, but one would have to sacrifice either a pair of steerer magnets or the phase intensity monitor cavity (PIMO) needed for finding the correct accelerating phase. Because of the high bunch charge of MESA stage-II increasing the length of the drifts is not an option.

The two pump setups then were altered so that the PIMO has a DN40 pumping port (see Fig. 1(c)). This port is screened by a sieve (compare Fig. 2), so there is no evanescent field leaking into the pipe. This maintains the radio frequency (RF) properties of the resonator and protects the IGP from RF.

SIMULATION & RESULTS

For the simulations baked surfaces of the stainless steel chambers of the beam pipe and the stub to the IGP are as-

* Work supported by DFG Cluster of Excellence "PRISMA+"

ISBN: 978-3-95450-227-1 ISSN: 2673-5490 doi:10.18429/JACoW-IPAC2022-THPOTK032

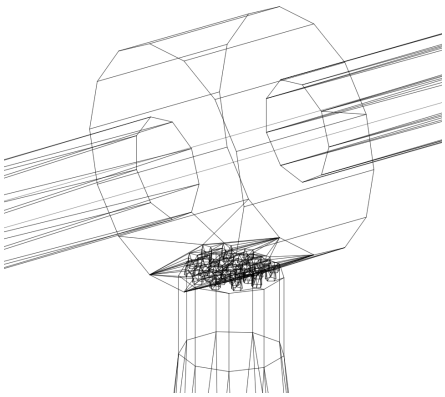

Figure 2: Sketch of a PIMO with a DN40 pumping port screened by a sieve.

sumed ($q_{\text{steel}} \approx 3 \times 10^{-12}$ mbar L/(cm^2 s), $T = 293.15$ K). The outgassing of the Cu surface of the RF sections was obtained by simulating the MAMBO prototype setup [12] with various outgassing parameters until the pressure found at the location of the IGP matched the experimental data. The value found was $q_{\text{Cu}} \approx 2 \times 10^{-10}$ mbar L/(cm^2 s) at $T = 313.15$ K. To mimic real IGP models the following port size and pumping speed combinations were used:

- $S_0 = 35$ L/s: DN40, DN63
- $S_0 = 60$ L/s: DN40, DN63, DN100
- $S_0 = 90$ L/s: DN100

It was also assumed, that MAMBO is separated from the rest of the accelerator vacuum system by closed valves in front of the first RF-section and ≈ 1 m behind the last one. Thus there is no additional pumping from the accelerator.

Each simulation job was run for ca. 10 min on an Intel Core i7 10750H CPU with 16 GB RAM. This resulted in already quite smooth pressure profiles. Runtimes of 1 h or more did not change the results significantly. Even after 2 min the results were already good enough to predict to what pressure a certain pumping speed or outgassing would lead.

The pressure profiles along MAMBO generated from the simulation results are shown in Figs. 3 and 4. From a configuration with four IGPs in total, i.e., the IGP behind the fourth RF-cavity is left out compared to what is shown in Fig. 1(a), one can see from Fig. 3 that the MAMBO cavities act like a differential pumping stage (red graph). Fig. 3 also shows the effect of increasing pumping speed and port cross section, both leading to better vacuum pressure. The most obvious increase in performance from larger cross sections can be found with the 35 L/s pumps in a configuration with one IGP per drift (5 IGPs). While for $S_0 = 60$ L/s there is not so much of a difference between DN63 and DN100. Also with a DN100 cross section there is not much of an improvement between a 60 L/s pump and one with $S_0 = 90$ L/s. The maximum pressure inside the RF-cavities ranges from

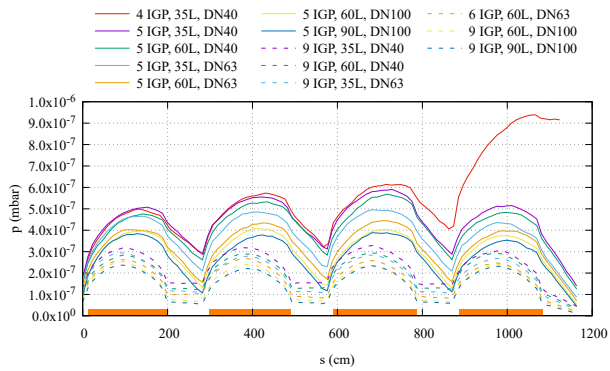

Figure 3: Pressure profiles of the configurations of the MAMBO vacuum system shown in Fig. 1(a) (solid) and Fig. 1(b) (dashed) for the investigated combinations of port size and pumping speed. The orange rectangles indicate the positions of the RF-cavities. The 4 IGP configuration is the one shown in Fig. 1(a) but with no pump behind the fourth cavity. Therefore the pressure in cavity four is higher by a factor of 2.

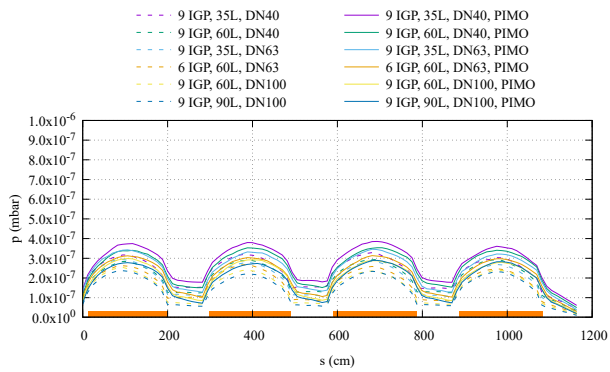

Figure 4: Comparison of the pressure profiles of the configurations shown in Fig. 1(b) (dashed) and Fig. 1(c) (solid) for the combinations of port sizes and pumping speeds under investigation. The orange rectangles indicate the positions of the RF-cavities. The reduction in cross section caused by the sieve increases the achievable pressure slightly.

3.8×10^{-7} mbar to 5.8×10^{-7} mbar. Using two pumps per drift reduces the respective values by a factor of 2.

In Fig. 4 pressure profiles with the pumps connected to the shielded PIMO are compared to unshielded ports. Because of the slightly reduced cross section of the RF-shielding the maximum vacuum pressure inside the MAMBO resonators is increases by ca. 0.5×10^{-7} mbar. This is acceptable given the gain of functionality from a PIMO inside of the drift.

From the results presented above the conclusion was drawn to use two IGPs per drift with a pumping speed of $S_0 = 60$ L/s and a DN63 cross section. The design of the MAMBO drifts was adapted accordingly.

ISBN: 978-3-95450-227-1 ISSN: 2673-5490 doi:10.18429/JACoW-IPAC2022-THPOTK032

SUMMARY

The MAMBO vacuum system was simulated with the Molflow+ code. Starting from an analytically estimated setup with only one small vacuum pump with a small cross section pumping port in front of each RF-cavity, simulations showed that surrounding each cavity with two larger pumps with increased port cross section is quite beneficial.

REFERENCES

[1] F. Hug *et al.*, "Status of the MESA ERL Project", in *Proc. 63rd Advanced ICFA Beam Dynamics Workshop on Energy Recovery Linacs (ERL'19)*, Berlin, Germany, Sep. 2019, pp. 14–17. doi:10.18429/JACoW-ERL2019-MOCOXBS05

[2] J. Teichert et al. "RF Status of Superconducting Module Development Suitable for CW Operation: ELBE Cryostats", *Nuclear Instruments and Methods in Physics Research Section A: Accelerators, Spectrometers, Detectors and Associated Equipment*, vol. 557, no. 1, 2006, pp. 239–242. doi:10.1016/j.nima.2005.10.077

[3] T. Stengler *et al.*, "Modified ELBE Type Cryomodules for the Mainz Energy-Recovering Superconducting Accelerator MESA", in *Proc. 17th Int. Conf. RF Superconductivity (SRF'15)*, Whistler, Canada, Sep. 2015, paper THPB116, pp. 1413–1416.

[4] T. Stengler *et al.*, "Status of the Superconducting Cryomodules and Cryogenic System for the Mainz Energy-recovering Superconducting Accelerator MESA", in *Proc. 7th Int. Particle Accelerator Conf. (IPAC'16)*, Busan, Korea, May 2016, pp. 2134–2137. doi:10.18429/JACoW-IPAC2016-WEPMB009

[5] R. Heine. "Preaccelerator concepts for an energy-recovering superconducting accelerator", *Phys.Rev.Accel.Beams*, vol. 24, no. 1, Jan 2021, pp. 011602. 10.1103/PhysRevAccelBeams.24.011602

[6] D.E. Nagle, E.A. Knapp, B.C. Knapp. "Coupled Resonator Model for Standing Wave Accelerator Tanks", *Review of Scientific Instruments*, vol. 38, no. 11, 1967, pp. 1583–1587. doi:10.1063/1.1720608

[7] E.A. Knapp, B.C. Knapp and J.M. Potter. "Standing Wave High Energy Linear Accelerator Structures", *Review of Scientific Instruments*, vol. 39, no. 7, 1968, pp. 979–991. doi:10.1063/1.1683583

[8] R. Kersevan and M. Ady, "Recent Developments of Monte-Carlo Codes Molflow+ and Synrad+", in *Proc. 10th Int. Particle Accelerator Conf. (IPAC'19)*, Melbourne, Australia, May 2019, pp. 1327–1330. doi:10.18429/JACoW-IPAC2019-TUPMP037

[9] D. Becker *et al.* "The P2 Experiment", *The European Physical Journal A*, vol. 54, no. 11, article 208, 2018. doi:10.1140/epja/i2018-12611-6

[10] S. Baunack. "Low Energy Accelerators for High Precision Measurements", Electromagnetic Interactions with Nucleons and Nuclei Conference (EINN20017), Paphos, Cyprus, Oct. 2017, http://einnconference.org/2017/presentations/01_Nov/W2/Baunack.pdf.

[11] N. Marquardt. "Introduction to the principles of vacuum physics", CERN Accelerator School Vacuum Technology, CERN-99-05, Snerkertsen, Denmark, May 1999, p.1. doi:10.5170/CERN-1999-005.1

[12] R. G. Heine, "Testing of the Milliampere Booster Prototype Cavity", in *Proc. 12th Int. Particle Accelerator Conf. (IPAC'21)*, Campinas, Brazil, May 2021, pp. 2693–2696. doi:10.18429/JACoW-IPAC2021-WEPAB041